Geophysical Research Letters®

Key Points:

- Maritime Continent deforestation has a potential to alter El Niño and La Niña complexities in spatial pattern and temporal evolutions
- Deforestation can strengthen subtropical El Niño-Southern Oscillation (ENSO) dynamics causing more Central Pacific and multi-year ENSOs
- The strengthened subtropical ENSO dynamics results from a deforestation-induced intensification of the mean northeastern Pacific high

The Potential Influence of Maritime Continent Deforestation on El Niño-Southern Oscillation: Insights From Idealized Modeling Experiments

Ting-Hui Lee[1,2], Jin-Yi Yu[1] , Yong-Fu Lin[1] , Min-Hui Lo[2] , and He-Ming Xiao[2]

[1]Department of Earth System Science, University of California, Irvine, Irvine, CA, USA, [2]Department of Atmospheric Sciences, National Taiwan University, Taipei, Taiwan

Abstract During the past two decades, the Maritime Continent (MC) has experienced increased deforestation. Here we show, with ensemble idealized deforestation experiments, that the MC deforestation could potentially alter the complexity (i.e., event-to-event differences) of the El Niño-Southern Oscillation (ENSO) in terms of its spatial pattern and temporal evolution. The deforestation model run increases the occurrences of the Central Pacific and multi-year types of ENSO compared to the control experiments. This change in ENSO complexity can be attributed to MC's intensification of the subtropical ENSO dynamics, commonly known as the seasonal footprinting mechanism. The deforestation amplifies the mean state of the subtropical high over the northeastern Pacific, leading to an increased dominance of subtropical ENSO dynamics in determining the ENSO pattern and evolution. This idealized coupled climate modeling study suggests that MC deforestation has a potential to alter ENSO's complexity, making El Niño more complex and less predictable.

Plain Language Summary This study examines how the deforestation in the maritime continent (MC) could induce a teleconnection that further alter the characteristics of El Niño-Southern Oscillation (ENSO). Using the fully-coupled Community Earth System Model, the researchers found that the sea level pressure over the North Pacific was strengthened in the idealized deforestation experiments. The anomalous high enhanced the air-sea coupling in the subtropical northeastern Pacific which can spread into the tropical Pacific to affect ENSO properties. Climate model simulations indicate that deforestation has the potential to increases the occurrence of Central Pacific (CP) and multi-year types of ENSO events compared to the control experiment. More CP and multi-year ENSO events increase the challenge of predicting the characteristics of ENSO and its global impacts. This study unveils that the potential of MC deforestation in alter ENSO properties, which could have potentially serious implications for society.

1. Introduction

Land-use changes are occurring globally (Hansen et al., 2013; Huang & Oey, 2019; Song et al., 2018) and can impact local and remote climates (Lawrence & Vandecar, 2015; Zhao et al., 2001). Deforestation is one of the common land-use changes, especially in tropical regions like the Maritime Continent (MC). Deforestation affects land properties such as surface albedo and roughness, impacting surface heat fluxes and radiation balance, leading to evapotranspiration decrease and surface temperature warming. These local effects can further impact land-atmosphere interactions, such as the land-sea breeze (Takahashi et al., 2017). Modeling studies have shown that deforestation in the MC region can affect local climate and circulations, resulting in an increase in local upward motion, moisture convergence, and precipitation (Chen et al., 2019; Huang & Oey, 2019; Wei et al., 2022).

MC deforestation's impact on local circulation can extend to influence regional and remote climate impacts. For instance, deforestation in the MC could contribute to precipitation decline over southern China by altering the tropical meridional circulation (Wei et al., 2022). MC deforestation can also lead to anomalous diabatic heating, which can then stimulate Rossby wave trains and result in remote impacts on extratropical climate (Delire et al., 2001; Schneck & Mosbrugger, 2011; Werth & Avissar, 2005), including a decline in the strength of Asia's summer monsoon (Huang & Oey, 2019).

Project Administration: Ting-Hui Lee, Jin-Yi Yu, Min-Hui Lo
Software: Ting-Hui Lee
Supervision: Jin-Yi Yu, Min-Hui Lo
Validation: Ting-Hui Lee, Yong-Fu Lin, He-Ming Xiao
Visualization: Ting-Hui Lee
Writing – original draft: Ting-Hui Lee, Jin-Yi Yu, Min-Hui Lo
Writing – review & editing: Ting-Hui Lee, Jin-Yi Yu, Yong-Fu Lin, Min-Hui Lo

The MC is situated the joint ascending branches of the Hadley and Walker circulations, making it susceptible to altering the basin-scale atmosphere-ocean couplings that drive the El Niño-Southern Oscillation (ENSO). Prior studies have explored the potential interactions between MC deforestation and ENSO (Lee & Lo, 2021; Meijide et al., 2018; Tölle et al., 2017), but have mainly focused on how ENSO modifies the climate impacts of MC deforestation, rather than how deforestation affects ENSO. In this study, we aim to examine the potential impact of MC deforestation on changing the properties of ENSO.

The Walker circulation plays a crucial role in the generation and development of ENSO, as it regulates the interactions between the tropical atmosphere and ocean. These interactions, as depicted by the Bjerknes feedback (Bjerknes, 1966, 1969) and charge-discharge process (Jin, 1997a, 1997b), involve surface wind, sea surface temperature (SST), and thermocline. Additionally, the Pacific's regional Hadley circulation, which ascends over the Indo-Pacific warm pool, including the MC, and descends over the northeastern Pacific, can also affect the ENSO generation and development through interactions between the subtropical Pacific ocean and atmosphere (Yu & Kim, 2011; Yu et al., 2010, 2012, 2017). The seasonal footprinting mechanism (Vimont et al., 2003; Yu & Fang, 2018) describes the specific process through which these interactions occur. The combination of these tropical ENSO dynamics (i.e., Walker circulation related tropical couplings) and subtropical ENSO dynamics (i.e, Hadley circulation related subtropical couplings) can result in varying characteristics of ENSO events, creating its complexity (Yu & Fang, 2018). These characteristics include the type of event, such as Eastern Pacific (EP) or Central Pacific (CP; Kao & Yu, 2009), and its temporal progression, which can be a single or multi-year event.

The study investigates the unexplored impact of MC deforestation on ENSO complexity through alternations in ENSO dynamics, achieved by conducting a series of idealized experiments. It is important to note that this modeling study primarily focuses on assessing hypothetical impacts rather than analyzing the effects resulting from existing deforestation activities.

2. Data, Method, and Experiments

The effects of MC deforestation on ENSO complexity were simulated using the fully-coupled Community Earth System Model version 1.2 (CESM1; Hurrell et al., 2013; see Text S1 in Supporting Information S1). Six paired simulations, consisting of control and deforestation runs, were conducted, each spanning 100 years of simulation time (Figure S1 in Supporting Information S1). In the control run, we prescribed the default plant functional types in the land model as the surface vegetation types across the MC. In the idealized deforestation experiments, the MC region's broadleaf evergreen and deciduous trees were entirely replaced with C4 grass (Figure S2 in Supporting Information S1), creating a maximum deforestation impact scenario. Additional details regarding the model and experiments can be found in Text S1 in Supporting Information S1.

ENSO events were identified by examining the area-averaged SST anomaly (SSTA) during the boreal winter over the cold tongue region. Anomalies here are defined as the deviations from the model climatology. An ENSO event was considered to occur in both the control and deforestation runs when the SSTA surpassed 0.7 standard deviations, a threshold determined based on the control run. In order to classify ENSO events as either EP- or CP-type, we conducted a comparative analysis of NIÑO3 and NIÑO4 indices. An ENSO event was categorized as an EP event when the NIÑO3 SST exceeded NIÑO4 SST, and vice versa. Additionally, we distinguished between single-year and multi-year ENSO events. A single-year ENSO event was identified when the SSTA returned to normal or transitioned to a different sign, whereas a multi-year event was identified when the same sign of SSTA was found in the subsequent winter. For additional details, please refer to Text S2 in Supporting Information S1.

3. Results

3.1. Changes in the Mean Climate State

The mean state differences between the ensemble deforestation and control runs indicate that MC deforestation leads to an increase in local land surface temperatures (Figure 1a) due to a decrease in evapotranspiration (Figure 1b). The increased land temperature strengthens land-sea contrast, causing anomalous moisture convergence and upward air motions (Figure 1c), resulting in an increase in precipitation (Figure 1d). We notice from Figure 1c that the enhanced ascending motion over the MC is accompanied by an enhanced descent over the ocean to the north and east, forming an anomalous local overturning circulation pattern. The existence of the
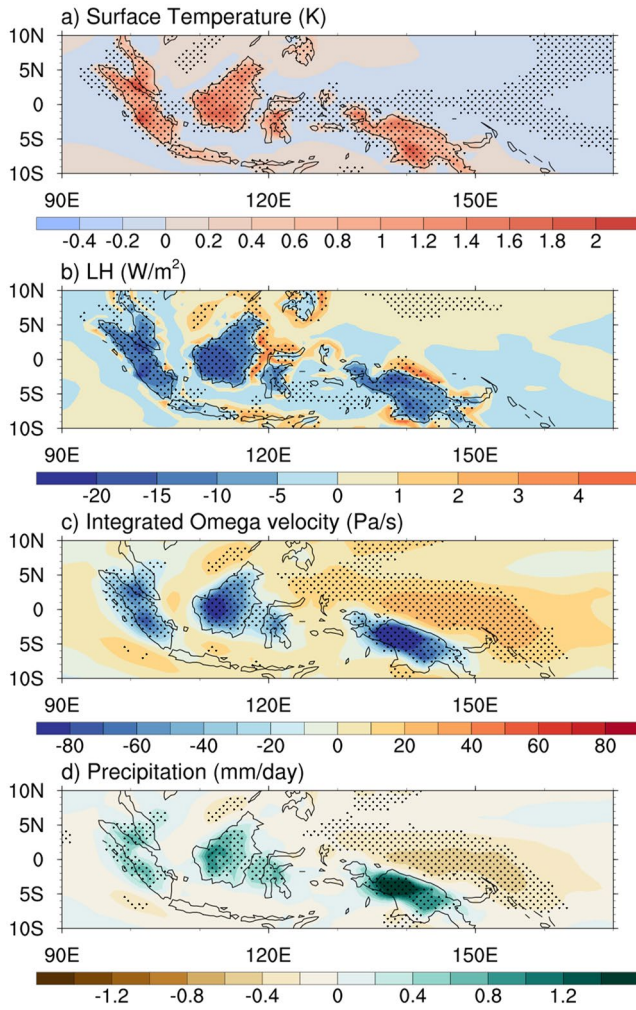
Figure 1. The annual mean state differences between the ensemble deforestation and control runs, including (a) surface temperature (in °C), (b) latent heat flux (in W/m²), (c) omega velocity (in Pa/s) integrated from 1,000 to 100 hPa with mass weighting, and (d) precipitation (in mm/day). The stippled areas indicate denote statistically significant at a 95% confidence level (student's t-test).

anomalous overturning is confirmed by a significant negative correlation, ranging from −0.31 to −0.52, between the yearly mean differences in ascending motion anomalies over the MC land (90–150°E, 10°S–10°N) and the descending motion anomalies over the ocean to the northeast of the MC (130–170°E, 7°S–4°N). Among the six pairs of experimental members, five of them demonstrate a significant negative correlation, with p-values below 0.001.

The deforestation-related overturning in the MC has the potential to alter the North Pacific's mean state. Based on the barotropic teleconnection mechanism proposed by Simmons et al. (1983), the perturbations in Southeast Asia may elicit responses in the North Pacific. We find that the descending branch of the overturning circulation suppresses convection within the tropical western Pacific (Figures 1c and 1d), resulting in anomalous diabatic heating over land and cooling over sea. This cooling process subsequently triggers the excitation of a Rossby wave train, which propagates poleward through the upper-troposphere (as shown in Figure 2a), akin to the mechanism described in Lee et al. (2009). Figure 2a illustrates the disparity in 200 hPa geopotential height between the deforestation and control runs, revealing that the wave train initially propagates northward to the central North Pacific and subsequently curves eastward toward North America. By examining the differences in geopotential height at various levels, namely 200, 500, 850 hPa, and sea level (as depicted in Figure S3 in Supporting Information S1), we have identified that the positive anomaly center of the wave train in the North Pacific exhibits a barotropic structure. This anomaly induces a positive difference in sea level pressure (SLP) over the subtropical northeastern Pacific (as illustrated in Figure 2c and Figure S3d in Supporting Information S1), which is the region where the climatological subtropical high is typically located during the boreal winter. The deforestation experiments imply MC deforestation's potential to enhance the North Pacific's subtropical high, which, in turn, may strengthen the subtropical ENSO dynamics.

We further employed a linear baroclinic model (LBM; Watanabe & Kimoto, 2000; see Text S1 in Supporting Information S1) to investigate the responses observed in the North Pacific during the CESM1 deforestation experiments. The LBM analysis reaffirms that the North Pacific responses observed are indeed stimulated by the anomalous descending branch of the deforestation-induced local overturning circulation in the northeastern region of MC (as depicted in Figures 2e–2j). In the LBM, we prescribed diabatic heating over land (Figure 2j) and cooling over the sea (Figure 2h), both of which engender a wave train, albeit with opposite signs, propagating toward the North Pacific (Figures 2g and 2i). However, the diabatic cooling over the sea dominates the wave train pattern due to its eastward positioning (Figure 2f). This cooling-induced forcing over the sea gives rise to a wave train in the North Pacific (Figure 2e) that closely resembles the wave train observed in the CESM1 experiment (Figure 2a). This similarity indicates that the atmospheric geopotential height responses in the CESM1 experiment, resulting from MC deforestation, can be predominantly explained by a linear dynamic response of the atmosphere to the deforestation-induced diabatic cooling to the northeast of MC. Note that the LBM's geopotential height response centers further west than CESM1, possibly due to the absence of nonlinear processes in the LBM model.

3.2. Changes in ENSO Complexity and Its Mechanisms

3.2.1. EP- and CP-Type ENSOs

Yu et al. (2015) suggested that a stronger mean state of the subtropical Pacific high should lead to a more efficient seasonal footprinting mechanism (i.e., the subtropical component of the ENSO dynamics), which should tend to produce the CP-type of ENSO (Yu et al., 2010; Yu & Kim, 2011). The seasonal footprinting mechanism
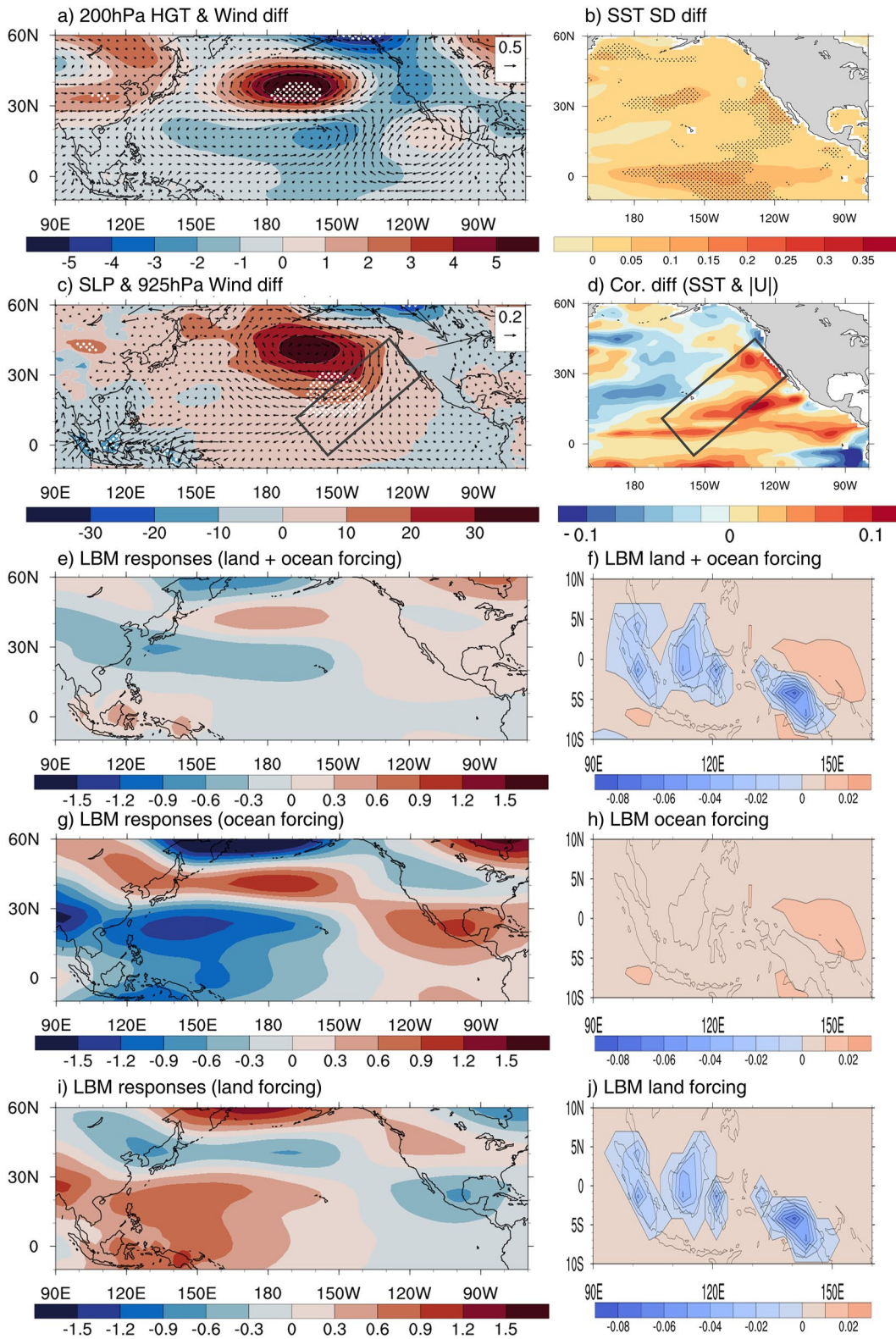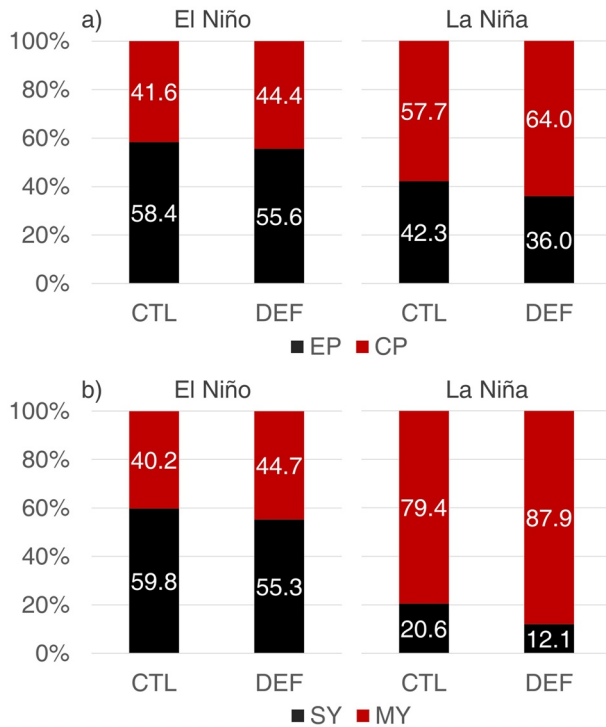
Figure 2.

Figure 3. The percentages of (a) the occurrence of tropical eastern Pacific (EP) and central Pacific (CP) and (b) the proportion of single-year (SY) and multi-year (MY) ENSO events in the control (CTL) and deforestation (DEF) ensemble simulations. The left (right) two bars correspond to El Niño (La Niña). EP/SY events are indicated in black, CP/MY events in red. See Tables S1 and S2 in Supporting Information S1 for detailed percentages.

proposes that a positive (negative) anomaly in trade winds in the northeastern Pacific can strengthen (weaken) local wind speeds, resulting in cooling down (warming up) of the underlying sea surface temperatures (SST) through the wind-evaporation-SST (WES) feedbacks (Xie & Philander, 1994). These SST anomalies in the subtropical Pacific can be sustained and propagate southward, eventually reaching the tropical central Pacific and triggering the Central Pacific (CP) type ESNO events (Kao & Yu, 2009). Yu et al. (2015) suggest that the effectiveness of this seasonal footprinting mechanism, or the strength of subtropical ENSO dynamics, increases (decreases) with a stronger (weaker) mean northeasterly trade wind component.

Given that MC deforestation has the potential to strengthen the mean trade winds over the northeastern Pacific (due to an increase in mean SLP compared to the control run), it is anticipated that the subtropical coupling associated with the seasonal footprinting mechanism will intensify under the MC deforestation scenario. Following Yu et al. (2015), we used the linear correlation coefficient between SST and 925 hPa zonal wind anomalies to quantify the air-sea coupling strength. Our analysis revealed a strengthening of air-sea coupling outside the coastline of Baha California following deforestation activities (the marked area in Figure 2d). This strengthening implies that the subtropical ENSO dynamics, which are known to favor the occurrence of CP-type ENSO (Yu & Kim, 2011; Yu et al., 2010, 2017), were amplified in the simulations involving MC deforestation. Consistent with this, we observed a significant increase in SST variance within the northeastern subtropical Pacific and the central tropical Pacific in the deforestation run compared to the control run (Figure 2b). Therefore, we may expect to see an increased occurrence of CP-type ENSO events in the deforestation run compared to the control run.

Our ensemble experiments show that ENSO complexity, in terms of spatial pattern changes, responds to MC deforestation. With the strengthening of the subtropical ENSO dynamics in the MC deforestation simulations, the percentage of CP-type El Niño events increases from 41.6% in the control run to 44.4% in the deforestation run (Figure 3a and Table S1 in Supporting Information S1). Considering the modest percentage increase, we conducted a bootstrap analysis to confirm the statistical significance of this rise (see Text S3 and Figure S4 in Supporting Information S1). Similarly, La Niña displays a higher dominance of the CP type, with the ensemble mean increasing from 57.7% in the control run to 64.0% in the deforestation run. In both the control and deforestation runs, La Niña events are consistently dominated by the CP-type. This is consistent with the general consensus in the ENSO research community that the existence of two types of ENSO spatial patterns (EP and CP) is more apparent for El Niño but not for La Niña (Capotondi et al., 2015; Paek et al., 2015). The observed La Niña events are known to be mostly of the CP-type than the EP-type. The cause of this El Niño-La Niña asymmetry is not yet fully understood, but one possible explanation is that the generation mechanism of La Niña may be more related to subtropical ENSO dynamics (e.g., Fan et al., 2023; Yu et al., 2023).

The percentage changes in the occurrence of CP- and EP-type ENSO following the MC deforestation exhibit modest variations in the ensemble mean, while larger changes are observed in each individual pair experiment. However, when examining the percentage changes within each individual ensemble member, three (four) out of the six members align with the ensemble-mean outcomes for El Niño (La Niña). By aggregating these favorable

Figure 2. (a)–(d) The differences between the ensemble deforestation and control runs. Panels (a)–(c) display the mean state differences in (a) wind (m/s) and geopotential height (HGT, in m) at 200 hPa, (b) standard deviation of sea surface temperature (°C), and (c) 925 hPa wind (m/s) and sea level pressure (SLP, in Pa). White stippling in (a) and (c) mark statistically significant SLP differences at 95% confidence (student's t-test). In (b), black stippling denotes significance at 90% confidence (f-test). Panel (d) presents the difference in the point-by-point sea surface temperature-zonal wind correlation between the ensemble deforestation and control run. The rectangle highlights the important area of strengthened subtropical ENSO dynamics. Panel (b) represents boreal winter differences (December to February), while (a), (c), and (d) cover boreal winter and spring (December to May). Panels (e) to (j) display the forcings (shown on the right side) and their corresponding responses (on the left side) in the LBM model. Panels (e), (g), and (i) present the resulting anomalous geopotential height at 200 hPa in response to (f) land and ocean forcing, (h) ocean forcing only, and (j) land forcing only, respectively.

members (i.e., those displaying an increased occurrence of CP-type ENSO events), the percentage increase of CP-type El Niño amounts to 11.7% (rising from 35.6% in the control run to 47.4% in the deforestation run), while for La Niña, the increase reaches 14.6% (ascending from 52.9% in the control run to 67.5% in the deforestation run).

3.2.2. Single- and Multi-Year ENSOs

Subtropical ENSO dynamics have the potential to generate multi-year events, whereas tropical ENSO dynamics typically result in single-year events (Yu & Fang, 2018). Yu and Fang (2018) propose that CP-type El Niño (La Niña) events can induce atmospheric wave trains that propagate into the northeastern Pacific. For instance, during a CP-type La Niña, there is an anomalous suppression of convection over the central Pacific, which can induce the development of an anomalous high over the subtropical north Pacific. This subsequently reactivates the seasonal footprinting mechanism and gives rise to another La Niña in the following year (Fang & Yu, 2020a), resulting in a multi-year La Niña event. In contrast, tropical ENSO dynamics, such as the charge-discharge mechanism, tend to produce single-year events due to a negative feedback loop. This feedback is driven by ENSO-induced thermocline variations in the tropical Pacific, causing an El Niño event to be followed by a La Niña event, and vice versa. Notably, a strong El Niño can discharge excessive equatorial Pacific Ocean heat content, potentially triggering multi-year La Niña events (Wu et al., 2019). However, recent investigations (Yu et al., 2023) suggest that most multi-year La Niña events are not necessarily originated from a preceding strong El Niño events. Instead, subtropical Pacific ENSO dynamics emerge as a more prominent mechanism for generating multi-year La Niña events.

We have demonstrated the strengthening of subtropical ENSO dynamics and an increased occurrence of CP-type ENSO events in the deforestation run. Consequently, it is expected that there will be a higher frequency of multi-year ENSO events as a result of MC deforestation.

In terms of the temporal evolution of ENSO, our findings show that the impact of MC deforestation is more pronounced for La Niña events compared to El Niño events. The percentage of multi-year La Niña events increases from 79.4% in the control run to 87.9% in the deforestation run (Figure 3b and Table S2 in Supporting Information S1; we discussed the overestimation of the multi-year La Niña events in model in Text S4 in Supporting Information S1). Additionally, five of the six ensemble members concur with the ensemble-mean results. By considering the favorable members (i.e., those exhibiting increased multi-year ENSO events), the percentage increase in multi-year La Niña events amounts to 13.8% (rising from 78.3% in the control run to 92.1% in the deforestation run, as shown in Table S2 in Supporting Information S1). As for multi-year El Niño events, their percentage increases from 40.2% to 44.7% after deforestation. Three of the six ensemble members display the same tendency of change as the ensemble mean. According to Fang and Yu (2020a), La Niña is more capable than El Niño in re-activating the positive feedback of the subtropical ENSO dynamics to produce multi-year events. Hence, when MC deforestation strengthens the subtropical ENSO dynamics, its impact on the occurrence of multi-year events is stronger for La Niña than El Niño. The ensemble of favorable members reveals that the percentage of multi-year El Niño events increases from 32.6% in the control run to 53.5% in the deforestation run. Overall, these results are consistent with the expected outcomes of intensified subtropical ENSO dynamics.

4. Summary and Discussion

In this idealized modeling study, MC deforestation is found to potentially alter ENSO complexity by enhancing the importance and dominance of subtropical ENSO dynamics. The underlying physical processes are outlined in Figure 4. Deforestation accompanies an anomalous local overturning circulation over the MC (step 1 in Figure 4), which triggers a wave train propagating toward the North Pacific and strengthens the SLP beneath it (step 2). This intensifies the background northeasterly winds over the northeastern Pacific, enhancing atmosphere-ocean interactions and the subtropical ENSO dynamics (step 3). Consequently, changes occur in the spatial pattern and temporal evolution of ENSO, with stronger subtropical ENSO dynamics in the deforestation scenario compared to the control scenario. This leads to an increase in the frequency of CP-type ESNO events (step 4) and the potential for more multi-year ENSO events due to the CP-type ENSO events' ability to further stimulate the subtropical ENSO dynamics (step 5).

Our results demonstrate that MC deforestation has the potential to alter the complexity of ENSO in its spatial pattern and temporal evolution. Given that La Niña already tends to be of the CP-type and multi-year (Fang & Yu, 2020b), the strengthened subtropical ENSO dynamics in the idealized MC deforestation simulations are likely
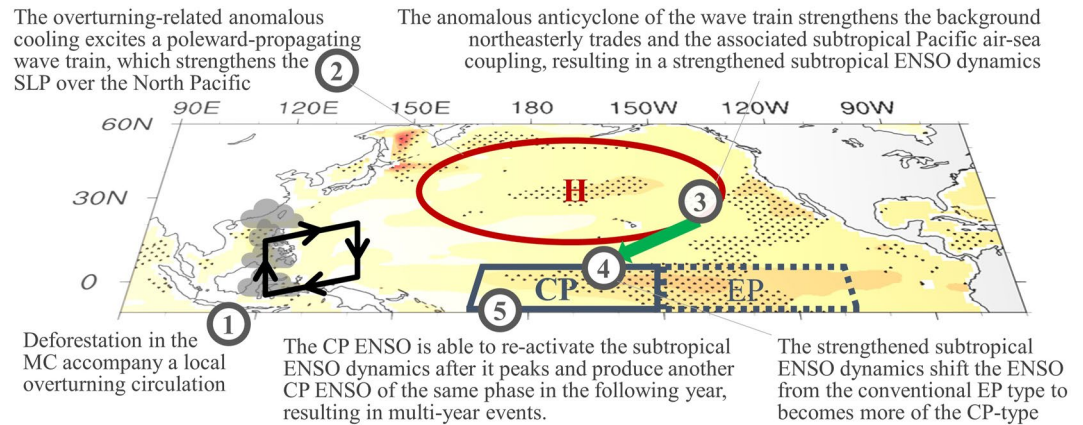
Figure 4. Key processes demonstrate MC deforestation's impact on atmospheric circulations and background states (1–3), ENSO dynamics in the subtropical region (3), SST variability during ENSO events (3), and ENSO complexity (4–5). Color shading represents SST variance differences (identical to Figure 2b).

to further enhance the dominance of these two specific patterns and evolution types. As a result, MC deforestation has the potential to further decrease the complexity of La Niña. However, MC deforestation is expected to shift the dominance of El Niño from the currently predominant EP-type and single-year toward a more frequent occurrence of the CP-type and multi-year. As a result, MC deforestation may result in an increase in El Niño complexity due to the amplification of stronger subtropical ENSO dynamics. This suggests that predicting El Niño events might be more difficult in a world affected by MC deforestation.

Yu et al. (2015) have indicated that the subtropical ENSO dynamics, which add complexity to ENSO, have gained greater significance in the 21st century. For example, multi-year La Niña events (such as the 2010-11-12, 2016-17-18, and 2020-21-22 events) appear to have become more frequent in the 21st century. Additionally, El Niño events have shifted from being single-year occurrences in the 20th century (e.g., 1982–1983 and 1997–1998 events) to being multi-year events (e.g., 2014-15-16 event). Previous studies have attributed the changing ENSO properties to global warming and decadal climate variability (Cai et al., 2018; Wen et al., 2020; Yu et al., 2017). Our study adds to this by suggesting that deforestation in the MC may also contribute to the growing complexity of ENSO by boosting the significance of subtropical ENSO dynamics. Further research is needed to investigate the effects of real-life deforestation in the MC, not just idealized scenarios.

Although our deforestation experiments are idealized and not realistic, they demonstrate the possibility that deforestation in the MC could increase the complexity of El Niño, making El Niño events more complex and harder to predict. The current study relies solely on the CESM1 numerical climate model, and the results may be subject to model dependence. Nevertheless, this study suggests that taking into account the new subtropical ENSO dynamics (Yu et al., 2017) may provide a deeper understanding of how deforestation in the MC may impact ENSO complexity.

Data Availability Statement

The restart and initial data for driving the CESM1 model, the surface data for driving the land model, and all figures and tables code are available on Zenodo (a software; https://zenodo.org/record/8358663). HadISST data can be downloaded at https://www.metoffice.gov.uk/hadobs/hadisst/data/download.html.

References

Bjerknes, J. (1966). A possible response of the atmospheric Hadley circulation to equatorial anomalies of ocean temperature. *Tellus*, *18*(4), 820–829. https://doi.org/10.1111/j.2153-3490.1966.tb00303.x

Bjerknes, J. (1969). Atmospheric teleconnections from the equatorial Pacific. *Monthly Weather Review*, *97*(3), 163–172. https://doi.org/10.1175/1520-0493(1969)097<0163:atftep>2.3.co;2

Cai, W., Wang, G., Dewitte, B., Wu, L., Santoso, A., Takahashi, K., et al. (2018). Increased variability of eastern Pacific El Niño under greenhouse warming. *Nature*, *564*(7735), 201–206. https://doi.org/10.1038/s41586-018-0776-9

Capotondi, A., Wittenberg, A. T., Newman, M., DiLorenzo, E., Yu, J.-Y., Braconnot, P., et al. (2015). Understanding ENSO diversity. *Bulletin of the American Meteorological Society*, *96*(6), 921–938. https://doi.org/10.1175/BAMS-D-13-00117.1

Chen, C.-C., Lo, M.-H., Im, E.-S., Yu, J.-Y., Liang, Y.-C., Chen, W.-T., et al. (2019). Thermodynamic and dynamic responses to deforestation in the maritime continent: A modeling study. *Journal of Climate*, *32*(12), 3505–3527. https://doi.org/10.1175/JCLI-D-18-0310.1

Delire, C., Behling, P., Coe, M. T., Foley, J. A., Jacob, R., Kutzbach, J., et al. (2001). Simulated response of the atmosphere-ocean system to deforestation in the Indonesian Archipelago. *Geophysical Research Letters*, *28*(10), 2081–2084. https://doi.org/10.1029/2000GL011947

Fan, H., Wang, C., & Yang, S. (2023). Asymmetry between positive and negative phases of the pacific meridional mode: A contributor to ENSO transition complexity. *Geophysical Research Letters*, *50*(14), e2023GL104000. https://doi.org/10.1029/2023GL104000

Fang, S.-W., & Yu, J.-Y. (2020a). A control of ENSO transition complexity by tropical Pacific mean SSTs through tropical-subtropical interaction. *Geophysical Research Letters*, *47*(12), e2020GL087933. https://doi.org/10.1029/2020GL087933

Fang, S.-W., & Yu, J.-Y. (2020b). Contrasting transition complexity between El Niño and La Niña: Observations and CMIP5/6 models. *Geophysical Research Letters*, *47*(16), e2020GL088926. https://doi.org/10.1029/2020GL088926

Hansen, M. C., Potapov, P. V., Moore, R., Hancher, M., Turubanova, S. A., Tyukavina, A., et al. (2013). High-resolution global maps of 21st-century forest cover change. *Science*, *342*(6160), 850–853. https://doi.org/10.1126/science.1244693

Huang, S., & Oey, L. (2019). Malay Archipelago forest loss to cash crops and urban expansion contributes to weaken the Asian Summer Monsoon: An atmospheric modeling study. *Journal of Climate*, *32*(11), 3189–3205. https://doi.org/10.1175/JCLI-D-18-0467.1

Hurrell, J. W., Holland, M. M., Gent, P. R., Ghan, S., Kay, J. E., Kushner, P. J., et al. (2013). The community Earth system model: A framework for collaborative research. *Bulletin of the American Meteorological Society*, *94*(9), 1339–1360. https://doi.org/10.1175/BAMS-D-12-00121.1

Jin, F.-F. (1997a). An equatorial ocean recharge paradigm for ENSO. Part I: Conceptual model. *Journal of the Atmospheric Sciences*, *54*(7), 811–829. https://doi.org/10.1175/1520-0469(1997)054<0811:AEORPF>2.0.CO;2

Jin, F.-F. (1997b). An equatorial ocean recharge paradigm for ENSO. Part II: A stripped-down coupled model. *Journal of the Atmospheric Sciences*, *54*(7), 830–847. https://doi.org/10.1175/1520-0469(1997)054<0830:AEORPF>2.0.CO;2

Kao, H.-Y., & Yu, J.-Y. (2009). Contrasting eastern-Pacific and central-Pacific types of ENSO. *Journal of Climate*, *22*(3), 615–632. https://doi.org/10.1175/2008JCLI2309.1

Lawrence, D., & Vandecar, K. (2015). Effects of tropical deforestation on climate and agriculture. *Nature Climate Change*, *5*(1), 27–36. https://doi.org/10.1038/nclimate2430

Lee, S.-K., Wang, C., & Mapes, B. E. (2009). A simple atmospheric model of the local and teleconnection responses to tropical heating anomalies. *Journal of Climate*, *22*(2), 272–284. https://doi.org/10.1175/2008JCLI2303.1

Lee, T.-H., & Lo, M.-H. (2021). The role of El Niño in modulating the effects of deforestation in the Maritime Continent. *Environmental Research Letters*, *16*(5), 54056. https://doi.org/10.1088/1748-9326/abe88e

Meijide, A., Badu, C. S., Moyano, F., Tiralla, N., Gunawan, D., & Knohl, A. (2018). Impact of forest conversion to oil palm and rubber plantations on microclimate and the role of the 2015 ENSO event. *Agricultural and Forest Meteorology*, *252*, 208–219. https://doi.org/10.1016/j.agrformet.2018.01.013

Paek, H., Yu, J.-Y., Hwu, J.-W., Lu, M.-M., & Gao, T. (2015). A source of AGCM bias in simulating the western Pacific subtropical high: Different sensitivities to the two types of ENSO. *Monthly Weather Review*, *143*(6), 2348–2362. https://doi.org/10.1175/MWR-D-14-00401.1

Schneck, R., & Mosbrugger, V. (2011). Simulated climate effects of Southeast Asian deforestation: Regional processes and teleconnection mechanisms. *Journal of Geophysical Research*, *116*(D11). D11116. https://doi.org/10.1029/2010JD015450

Simmons, A. J., Wallace, J. M., & Branstator, G. W. (1983). Barotropic wave propagation and instability, and atmospheric teleconnection patterns. *Journal of the Atmospheric Sciences*, *40*(6), 1363–1392. https://doi.org/10.1175/1520-0469(1983)040<1363:BWPAIA>2.0.CO;2

Song, X.-P., Hansen, M. C., Stehman, S. V., Potapov, P. V., Tyukavina, A., Vermote, E. F., & Townshend, J. R. (2018). Global land change from 1982 to 2016. *Nature*, *560*(7720), 639–643. https://doi.org/10.1038/s41586-018-0411-9

Takahashi, A., Kumagai, T., Kanamori, H., Fujinami, H., Hiyama, T., & Hara, M. (2017). Impact of tropical deforestation and forest degradation on precipitation over Borneo Island. *Journal of Hydrometeorology*, *18*(11), 2907–2922. https://doi.org/10.1175/JHM-D-17-0008.1

Tölle, M. H., Engler, S., & Panitz, H.-J. (2017). Impact of abrupt land cover changes by tropical deforestation on Southeast Asian climate and agriculture. *Journal of Climate*, *30*(7), 2587–2600. https://doi.org/10.1175/JCLI-D-16-0131.1

Vimont, D. J., Wallace, J. M., & Battisti, D. S. (2003). The seasonal footprinting mechanism in the Pacific: Implications for ENSO. *Journal of Climate*, *16*(16), 2668–2675. https://doi.org/10.1175/1520-0442(2003)016<2668:TSFMIT>2.0.CO;2

Watanabe, M., & Kimoto, M. (2000). Atmosphere-ocean thermal coupling in the North Atlantic: A positive feedback. *Quarterly Journal of the Royal Meteorological Society*, *126*(570), 3343–3369. https://doi.org/10.1002/qj.49712657017

Wei, S., Wang, X., & Xie, Q. (2022). Strengthening effect of Maritime Continent deforestation on the precipitation decline over southern China during late winter and early spring. *Climate Dynamics*, *60*(3–4), 1173–1185. https://doi.org/10.1007/s00382-022-06362-6

Wen, Q., Döös, K., Lu, Z., Han, Z., & Yang, H. (2020). Investigating the role of the Tibetan Plateau in ENSO variability. *Journal of Climate*, *33*(11), 4835–4852. https://doi.org/10.1175/JCLI-D-19-0422.1

Werth, D., & Avissar, R. (2005). The local and global effects of Southeast Asian deforestation. *Geophysical Research Letters*, *32*(20), L20702. https://doi.org/10.1029/2005GL022970

Wu, X., Okumura, Y. M., & DiNezio, P. N. (2019). What controls the duration of El Niño and La Niña events? *Journal of Climate*, *32*(18), 5941–5965. https://doi.org/10.1175/JCLI-D-18-0681.1

Xie, S.-P., & Philander, S. G. H. (1994). A coupled ocean-atmosphere model of relevance to the ITCZ in the eastern Pacific. *Tellus A: Dynamic Meteorology and Oceanography*, *46*(4), 340–350. https://doi.org/10.3402/tellusa.v46i4.15484

Yu, J.-Y., & Fang, S.-W. (2018). The distinct contributions of the seasonal footprinting and charged-discharged mechanisms to ENSO complexity. *Geophysical Research Letters*, *45*(13), 6611–6618. https://doi.org/10.1029/2018GL077664

Yu, J.-Y., Kao, H.-Y., & Lee, T. (2010). Subtropics-related interannual sea surface temperature variability in the central equatorial Pacific. *Journal of Climate*, *23*(11), 2869–2884. https://doi.org/10.1175/2010JCLI3171.1

Yu, J.-Y., Kao, P., Paek, H., Hsu, H.-H., Hung, C., Lu, M.-M., & An, S.-I. (2015). Linking emergence of the central Pacific El Niño to the Atlantic multidecadal oscillation. *Journal of Climate*, *28*(2), 651–662. https://doi.org/10.1175/JCLI-D-14-00347.1

Yu, J.-Y., Kim, J.-W., Zhu, T., & Lin, Y.-F. (2023). Exploring the formation of multi-year la niña events through tropical and subtropical ENSO dynamics and their distinct climate effects. In *28th general assembly of the international union of geodesy and geophysics (IUGG) (Berlin 2023)*. https://doi.org/10.57757/IUGG23-2478

Yu, J.-Y., & Kim, S. T. (2011). Relationships between extratropical sea level pressure variations and the central Pacific and eastern Pacific types of ENSO. *Journal of Climate*, *24*(3), 708–720. https://doi.org/10.1175/2010JCLI3688.1

Yu, J.-Y., Lu, M.-M., & Kim, S. T. (2012). A change in the relationship between tropical central Pacific SST variability and the extratropical atmosphere around 1990. *Environmental Research Letters*, *7*(3), 34025. https://doi.org/10.1088/1748-9326/7/3/034025

Yu, J.-Y., Wang, X., Yang, S., Paek, H., & Chen, M. (2017). The changing El Niño–Southern Oscillation and associated climate extremes. *Climate extremes* (pp. 1–38). https://doi.org/10.1002/9781119068020.ch1

Zhao, M., Pitman, A. J., & hase, T. (2001). The impact of land cover change on the atmospheric circulation. *Climate Dynamics*, *17*(5), 467–477. https://doi.org/10.1007/PL00013740

References From the Supporting Information

Bonan, G. B., Levis, S., Kergoat, L., & Oleson, K. W. (2002). Landscapes as patches of plant functional types: An integrating concept for climate and ecosystem models. *Global Biogeochemical Cycles*, *16*(2), 5–23. https://doi.org/10.1029/2000GB001360

Carlson, K. M., Curran, L. M., Ratnasari, D., Pittman, A. M., Soares-Filho, B. S., Asner, G. P., et al. (2012). Committed carbon emissions, deforestation, and community land conversion from oil palm plantation expansion in West Kalimantan, Indonesia. *Proceedings of the National Academy of Sciences of the United States of America*, *109*(19), 7559–7564. https://doi.org/10.1073/pnas.1200452109

Deser, C., Knutti, R., Solomon, S., & Phillips, A. S. (2012). Communication of the role of natural variability in future North American climate. *Nature Climate Change*, *2*(11), 775–779. https://doi.org/10.1038/nclimate1562

Hunke, E. C., & Lipscomb, W. H. (2015). CICE: The Los Alamos sea ice model documentation and software user's manual version 5.1 LA-CC-06-012. Retrieved from https://svn-ccsm-models.cgd.ucar.edu/cesm1/alphas/branches/cesm1_5_alpha04c_timers/components/cice/src/doc/cicedoc.pdf

Kim, J.-W., & Yu, J.-Y. (2022). Single- and multi-year ENSO events controlled by pantropical climate interactions. *Npj Climate and Atmospheric Science*, *5*(1), 88. https://doi.org/10.1038/s41612-022-00305-y

Lawrence, D. M., Oleson, K. W., Flanner, M. G., Thornton, P. E., Swenson, S. C., Lawrence, P. J., et al. (2011). Parameterization improvements and functional and structural advances in version 4 of the community land model. *Journal of Advances in Modeling Earth Systems*, *3*(1), M03001. https://doi.org/10.1029/2011MS00045

Neale, R. B., Chen, C. C., Gettelman, A., Lauritzen, P. H., Park, S., Williamson, D. L., et al. (2010). *Description of the NCAR community atmosphere model: CAM5.0. NCAR technical note*. National Center for Atmospheric Research. Retrieved from https://www2.cesm.ucar.edu/models/cesm1.2/cam/docs/description/cam5_desc.pdf

Oleson, K. W., Lawrence, D. M., Bonan, G. B., Flanner, M. G., Kluzek, E., Lawrence, P. J., et al. (2010). *Technical description of version 4.0 of the community land model (CLM) (No. NCAR/TN-478+STR)*. University Corporation for Atmospheric Research. Retrieved from https://opensky.ucar.edu/islandora/object/technotes%3A493/datastream/PDF/view

Rayner, N. A., Parker, D. E., Horton, E. B., Folland, C. K., Alexander, L. V., Rowell, D. P., et al. (2003). Global analyses of sea surface temperature, sea ice, and night marine air temperature since the late nineteenth century. *Journal of Geophysical Research*, *108*(D14). 4407. https://doi.org/10.1029/2002JD002670

Smith, R., Jones, P., Briegleb, B., Bryan, F., Danabasoglu, G., Dennis, J., et al. (2010). The parallel ocean program (POP) reference manual, ocean component of the community climate System model (CCSM), LANL tech. Report, LAUR-10-01853 (p. 141). Retrieved from https://www2.cesm.ucar.edu/models/cesm1.0/pop2/doc/sci/POPRefManual.pdf

Sriver, R. L., Forest, C. E., & Keller, K. (2015). Effects of initial conditions uncertainty on regional climate variability: An analysis using a low-resolution CESM ensemble. *Geophysical Research Letters*, *42*(13), 5468–5476. https://doi.org/10.1002/2015GL064546